

# Radiation from Fine Particle Clouds in High-Temperature Combustion Gas

By

Takashi SATO\* and Takeshi KUNITOMO\*

(Received September 22, 1964)

Radiation from fine particle cloud floating in high-temperature combustion gas was studied theoretically and the effects of temperature, its distribution, absorption thickness and the distribution of volumetric concentration were made clear. Radiations from particle clouds of carbon, ferric oxide, converter ash, diatomaceous earth and boiler ash were measured and the emissivity of particle cloud which has equal absorption thickness decreases in the following order of carbon, ferric oxide, converter ash, diatomaceous earth and boiler ash. The order of these emissivities agreed with that of the emissivities of particle-piled surfaces. Empirical formulae were obtained for the relation between the emissivity and absorption thickness.

## 1. Introduction

With the progress of steam power plants, the proportion of the radiative heat transfer surface in the total heat transfer surface is increasing, and that of the convective heat transfer surface is on the contrary decreasing. However, the mechanism of radiative heat transfer from luminous flame including soot has not yet been made clear. Besides, in the case of other industrial furnaces, that is blast furnace, open hearth furnace, converter and etc., radiative heat transfer from fine particle clouds floating in combustion gas or high-temperature exhaust gas has not yet been studied either.

In the present paper, the relationship between the radiative intensity or the emissivity of fine particle cloud floating in high-temperature gas and its mean temperature, temperature distribution, absorption thickness and the distribution of volumetric concentration was obtained theoretically. And experimental work was performed as follows. Various kinds of luminous flame were made by inserting several fine particles into the perfectly burnt town gas flame. Mean flame temperature and radiative intensity of certain section

---

\* Department of Mechanical Engineering

of these luminous flames were measured and then emissivities of fine particle clouds themselves were calculated using the proper method.

## 2. Theory of Radiation from Particle Cloud Floating in High-Temperature Gas

The assumption introduced was that the absorption coefficient of fine particle cloud is independent of temperature and the absorptivity is equal to the emissivity.

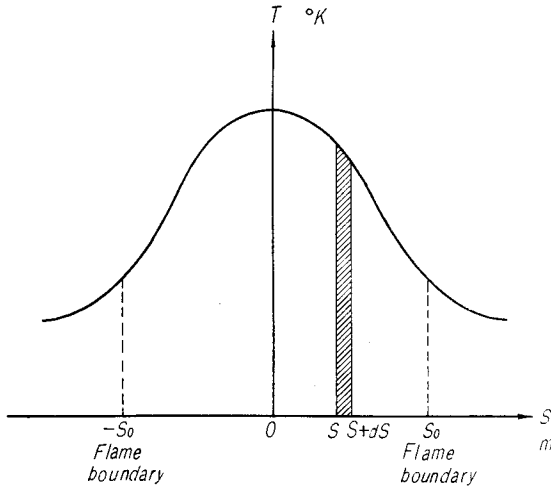


Fig. 1.

In the fine particle cloud which has the temperature distribution shown in Fig. 1, the monochromatic absorptivity of particle cloud in infinitesimal small length  $dS$  can be written in the following form by Beer's law,

$$1 - e^{-\delta_\lambda v(S)dS}, \quad (1)$$

where  $\delta_\lambda$  is the monochromatic absorption coefficient of particle cloud and  $v(S)$  is the volumetric concentration of particle at the distance  $S$ . As  $\delta_\lambda v(S)dS$

is a very small value, the above value is approximately equal to

$$\delta_\lambda v(S)dS.$$

As the emissivity is assumed to be equal to the absorptivity, the monochromatic radiative intensity of the cloud in infinitesimal small length  $dS$  is estimated by the following equation by the application of Planck's radiation law,

$$\frac{1}{\pi} \cdot \frac{C_1 \lambda^{-5}}{e^{C_2/\lambda T(S)} - 1} \cdot \delta_\lambda v(S)dS \quad (2)$$

where  $C_1$  and  $C_2$  are Planck's dimensional constants,  $\lambda$  is the wave length and  $T(S)$  is the temperature at the distance  $S$ . As this radiative intensity is weakened by the particle cloud included in the depth between  $S$  and  $S_0$ , the intensity which transmits to the outside of the cloud is estimated as

$$\frac{1}{\pi} \cdot \frac{C_1 \lambda^{-5}}{e^{C_2/\lambda T(S)} - 1} \cdot \delta_\lambda v(S)dS \cdot e^{-\int_S^{S_0} \delta_\lambda v(S)dS}. \quad (3)$$

For the whole wave length, the radiative intensity is

$$\int_0^{\infty} \frac{1}{\pi} \cdot \frac{C_1 \lambda^{-5}}{e^{C_2/\lambda T(S)} - 1} \cdot \delta_{\lambda} v(S) dS \cdot e^{-\int_{S_0}^{\infty} \delta_{\lambda} v(S) dS} d\lambda. \quad (4)$$

Hence, the total radiative intensity from the whole part of the cloud is

$$J_n = \int_{-S_0}^{S_0} v(S) dS \int_0^{\infty} \frac{1}{\pi} \cdot \frac{C_1 \lambda^{-5}}{e^{C_2/\lambda T(S)} - 1} \cdot \delta_{\lambda} \cdot e^{-\int_{S_0}^{\infty} \delta_{\lambda} v(S) dS} d\lambda. \quad (5)$$

The radiative intensity  $J_n$  can be calculated if the monochromatic absorption coefficient  $\delta_{\lambda}$  is known as a function of wave length  $\lambda$ .

In the case of soot and carbon, the monochromatic absorption coefficient  $\delta_{\lambda}$  is found to be  $k/\lambda^{\alpha}$ , where  $k$  is constant, and  $\alpha$  is also constant which is equal to 1 approximately<sup>1)</sup>. But in the case of the other particle,  $\delta_{\lambda}$  is not known in detail. However, in the present paper,  $\delta_{\lambda}$  is assumed to be  $k/\lambda$  for all kinds of particle for simplicity.

Substitution of  $\delta_{\lambda} = k/\lambda$  into Eq. (5) gives

$$J_n = \frac{kC_1}{\pi} \int_{-S_0}^{S_0} v(S) dS \int_0^{\infty} \frac{\lambda^{-6}}{e^{C_2/\lambda T(S)} - 1} \cdot e^{-(k/\lambda) \int_{S_0}^{\infty} v(S) dS} d\lambda. \quad (6)$$

Then, substituting  $a(S) = C_2/T(S)$ ,  $b(S) = k \int_{S_0}^{\infty} v(S) dS$  and  $a/\lambda = t$ , we obtain

$$\begin{aligned} J_n &= \frac{kC_1}{\pi} \int_{-S_0}^{S_0} v(S) dS \cdot \frac{1}{a^5} \cdot \int_0^{\infty} \frac{t^4 e^{-(b/a)t}}{e^t - 1} dt \\ &= \frac{kC_1}{\pi} \int_{-S_0}^{S_0} v(S) dS \cdot \frac{1}{a^5} \cdot \int_0^{\infty} \frac{t^4 e^{-(b/a+1)t}}{1 - e^{-t}} dt \\ &= -\frac{kC_1}{C_2^5 \pi} \int_{-S_0}^{S_0} v(S) T^5(S) \psi^{(4)}(x+1) dS, \end{aligned} \quad (7)$$

where  $x \equiv \frac{b}{a} = kT(S) \int_0^{S_0} v(S) dS / C_2$  and  $\psi^{(4)}(x)$  is Hexa-gamma function.

Substitution of

$$\psi^{(4)}(x+1) = -24 \sum_{n=1}^{\infty} 1/(x+n)^5 \quad (8)$$

and

$$s = S/S_0 \quad (9)$$

into Eq. (7) gives

$$\begin{aligned} J_n &= \frac{24kC_1}{C_2^5 \pi} \int_{-S_0}^{S_0} v(S) T^5(S) \left\{ \sum_{n=1}^{\infty} t/(x+n)^5 \right\} dS \\ &= \frac{24kC_1 S_0}{C_2^5 \pi} \int_{-1}^1 v(s) T^5(s) \left\{ \sum_{n=1}^{\infty} 1/(x+n)^5 \right\} ds, \end{aligned} \quad (10)$$

where  $x = kS_0 T(s) \int_s^1 v(s) ds / C_2$

The above equation is difficult to solve in the case of complicated distribution of temperature and volumetric concentration. For simplicity the temperature distribution is assumed to be

$$T(s) = T_0(1-g|s|), \quad g = \text{const.} \quad (11)$$

and the distribution of volumetric concentration is assumed to be

$$v(s) = v_0(1-f|s|), \quad f = \text{const.}, \quad (12)$$

as shown in Fig. 2.

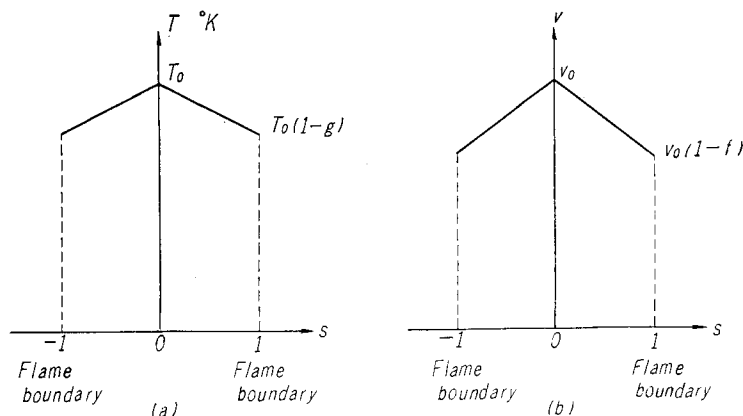


Fig. 2.

If the approximation

$$\sum_{n=1}^{\infty} 1/(x+n)^5 \doteq px^3 + qx^2 + rx + c,$$

where  $p$ ,  $q$ ,  $r$  &  $c$  are constants, is possible and is substituted into Eq. (10), integration can easily be carried out. The results of the above calculation are shown in Fig. 3 and 4. In this calculation, mean temperature  $T_m$ , mean volumetric concentration  $v_m$ , theoretical emissivity  $\varepsilon_{th}$  and the variable  $x_m$  are defined respectively as follows,

$$T_m = T_0 \left(1 - \frac{g}{2}\right), \quad (13)$$

$$v_m = v_0 \left(1 - \frac{f}{2}\right), \quad (14)$$

$$\varepsilon_{th} = \frac{Jn}{\frac{\sigma T_m^4}{\pi}}, \quad \text{where } \sigma = C_1 \pi^4 / C_2^5 \cdot 15 \quad (15)$$

and

$$x_m = 2kT_m v_m S_0 / C_2, \quad (16)$$

where in this case  $2v_m S_0$  represents the absorption thickness.

In the special case of  $g=0$  and  $f=0$ , the following results are easily obtained<sup>2)</sup>.

$$Jn = -\frac{kC_1}{C_2^5 \pi} \cdot v_m T_m \int_{-S_0}^{S_0} \psi^{(4)}(x+1) dx, \quad (17)$$

where  $x = kT_m v_m (S_0 - S) / C_2$ .

Substitution of  $dx = -kT_m v_m dS / C_2$  into Eq. (17) gives

$$\begin{aligned}
 J_n &= \frac{C_1 T_m^4}{C_2^4 \pi} \int_{2kT_m v_m S_0 / C_2}^0 \psi^{(4)}(x+1) dx \\
 &= \frac{C_1 T_m^4}{C_2^4 \pi} \left\{ \psi^{(3)}(1) - \psi^{(3)}\left(\frac{2kT_m v_m S_0}{C_2} + 1\right) \right\} \\
 &= \frac{C_1 \pi^4}{C_2^4 15} \cdot \frac{T_m^4}{\pi} \left\{ 1 - \frac{15}{\pi^4} \psi^{(3)}(x_m + 1) \right\} \\
 &= \sigma \cdot \frac{T_m^4}{\pi} \left\{ 1 - \frac{15}{\pi^4} \psi^{(3)}(x_m + 1) \right\}, \tag{18}
 \end{aligned}$$

where  $x_m = 2kT_m v_m S_0 / C_2$ , and  $\psi^{(3)}(x)$  is Penta-gamma function. Then the theoretical emissivity  $\epsilon_{th}$  is calculated as follows.

$$\epsilon_{th} = 1 - \frac{15}{\pi^4} \psi^{(3)}(x_m + 1) \tag{19}$$

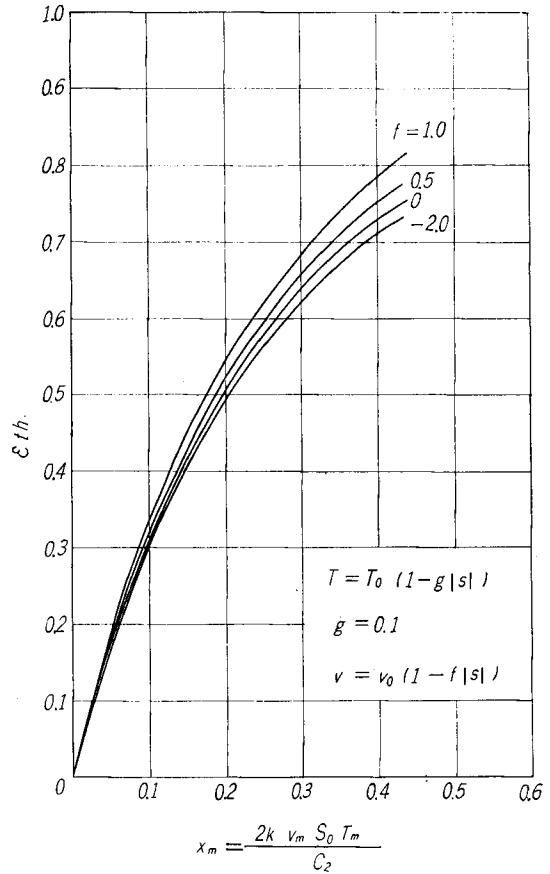
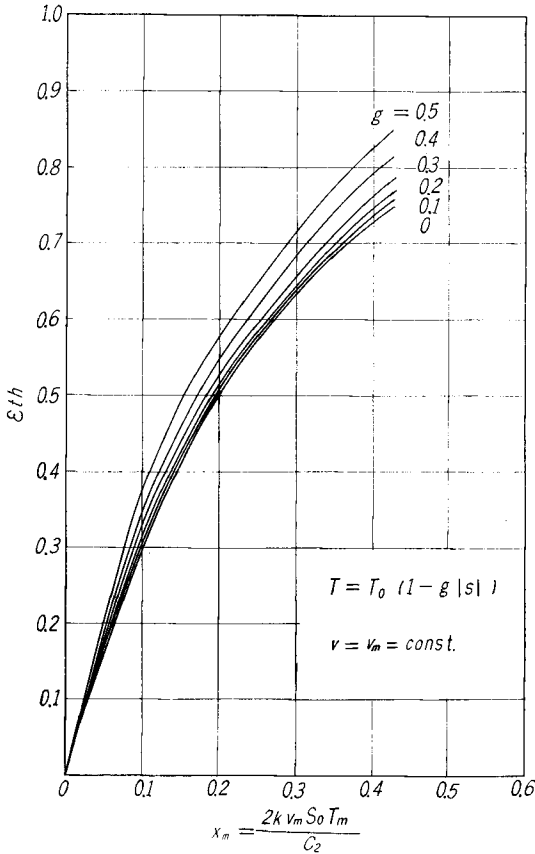


Fig. 3. The relation between the theoretical emissivity and the variable  $x_m$ . The effect of the temperature distribution.

Fig. 4 a.

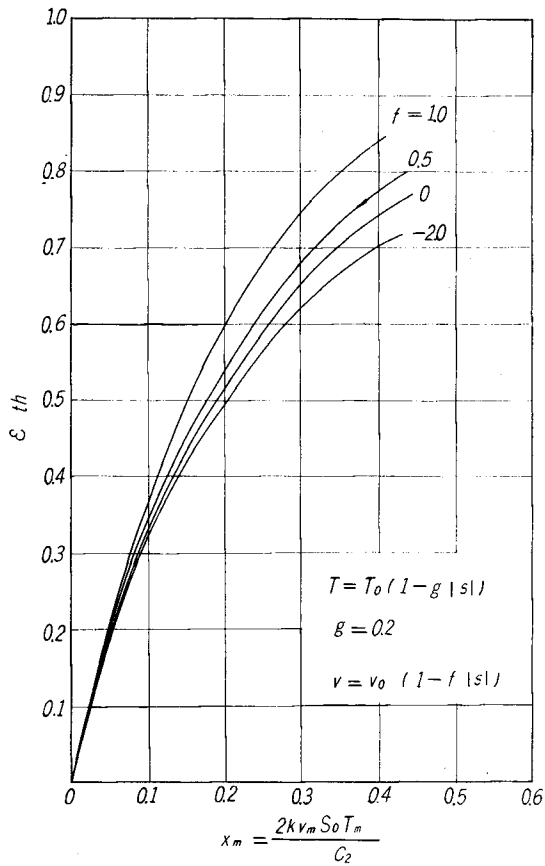


Fig. 4 b.

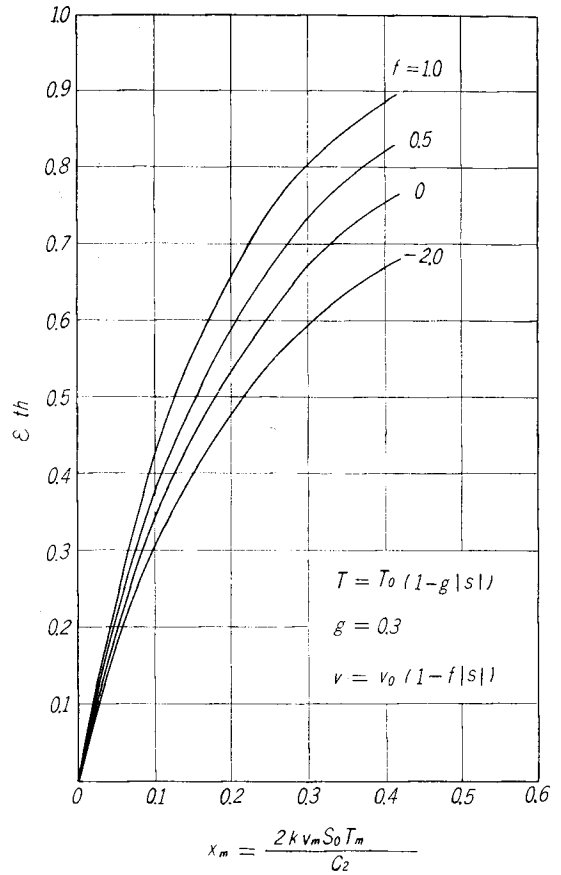


Fig. 4 c.

Fig. 4. The relation between the theoretical emissivity and the variable  $x_m$ . The effect of the distribution of volumetric concentration.

As recognized from each figure, when the temperature distribution is fixed, the emissivity of the cloud, which distributes more richly in the central high-temperature region of the flame, is higher than that of the cloud which distributes more richly in the circumferential low-temperature region of the flame. And when the mean volumetric concentration of particle is fixed, the influence of the distribution of volumetric concentration becomes more remarkable according as the temperature distribution becomes sharper. But the differences among them are not so large as shown in Fig. 3 & 4.

### 3. Experimental Equipment and Procedure

An explanatory sketch of experimental arrangement is shown in Fig. 5. Combustion chamber had a cylindrical form of inside diameter 300 mm and

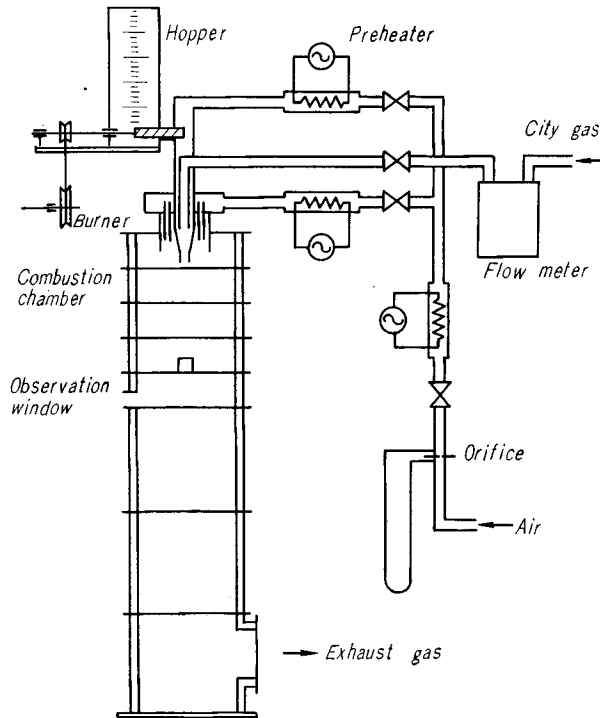


Fig. 5. The explanatory sketch of experimental arrangement.

height 1500 mm. A gas burner was equipped on the top of the furnace. Furnace wall was cooled by water and covered with thin soot layer, so the absorptivity of radiation of this wall was considered 1. Town gas was guided to the burner after measured its flow rate by a flow meter and combustion air was sent by a blower to the burner after passing through an orifice and the preheating zones. Regulating the flow rate of combustion air, town gas could burn perfectly. Then the temperature of this non-luminous flame was measured by the naked PtRh(20)-PtRh(5) thermocouple inserted from the observation window.

As the absorptivity of furnace wall is equal to 1, the equation of heat balance concerning the thermocouple

$$\alpha(T_g - T) + \epsilon \epsilon'_g \sigma T_g^4 = \epsilon \sigma T^4$$

can be applied approximately, where  $T$  is the temperature of combustion gas,  $\alpha$  is the convective heat transfer coefficient from combustion gas to the thermocouple,  $\epsilon$  is the emissivity of the thermocouple surface,  $\epsilon'_g$  is the emissivity of combustion gas surrounding the thermocouple, and  $\sigma$  is the Stefan-Boltzmann's

constant. Using this equation, the temperature of combustion gas can be calculated from the measured value of thermocouple temperature.

Using the radiation pyrometer, the blackbody temperature of combustion gas  $T_{gb}$  was measured, then the radiative intensity of this non-luminous flame can be estimated as  $\sigma T_{gb}^4/\pi$ . As the radiative intensity of blackbody which has the mean temperature  $T_{gm}$  of combustion gas is  $\sigma T_{gm}^4/\pi$ , the emissivity  $\varepsilon_g$  of the non-luminous flame can be calculated as follows.

$$\varepsilon_g = (T_{gb}/T_{gm})^4$$

In the next step, fine particles were inserted from the hopper by the screw conveyer into this non-luminous flame, then the luminous flame originated. The mean temperature  $T_{pm}$  and the blackbody temperature  $T_{pb}$  of the luminous flame being measured in the same way, the emissivity  $\varepsilon_t$  of the luminous flame can be calculated by the following equation

$$\varepsilon_t = (T_{pb}/T_{pm})^4.$$

The temperature difference between the fine particle and the surrounding gas was estimated as 1°C at most, using the Heisler chart<sup>3)</sup>. Then  $T_{pm}$  also shows the mean temperature of particle cloud.

Assuming that the composition of gases of the measuring part of the flame is not changed by mixing particles, the emissivity  $\varepsilon_p$  of the particle cloud itself can be calculated as follows:

$$\begin{aligned}\varepsilon_t &= 1 - (1 - \varepsilon_g)(1 - \varepsilon_p) \\ \varepsilon_p &= 1 - \{(1 - \varepsilon_t)/(1 - \varepsilon_g)\}\end{aligned}$$

When the mean temperature of the luminous flame was high enough, the two-colour filter method using the optical pyrometer was carried out in addition. The difference between the mean temperature taken by the naked thermocouple method and that taken by the above optical method was very small, that is 0°C~10°C.

The volume of the particle cloud in a unit volume of combustion gas  $v_m(m^3/m^3)$  was calculated by the following equation, using the amount of consumption of particles in the hopper  $w(m^3/s)$  and the flow rate of combustion gas  $G(m^3/s)$  which was able to be estimated from the temperature of the measuring part and the flow rate of air and town gas.

$$v_m = w/G$$

And, in order to calculate the absorption thickness of particle cloud  $v_m S_0(m)$ , the observed breadth  $S_0$  was determined as the range where the flame reaction of sodium was observed.



Especially in the experiment of carbon particle, the emissivity and the volumetric concentration  $v_m$  are compensated by the results of gas analysis, since it must be taken in consideration that the particles are somewhat consumed by the combustion of particles themselves.

#### 4. Experimental Results

##### (1) Properties of fine particles used

Particles used were carbon, the ash of boiler (main component ;  $\text{SiO}_2$ ,  $\text{Al}_2\text{O}_3$ ), ferric oxide  $\text{Fe}_2\text{O}_3$ , the ash of converter (main component ;  $\text{Fe}_2\text{O}_3$ ) and diatomaceous earth. The diameter distributions of these particles measured by the projection of microscopic photographs are shown in Fig. 6. And the specific

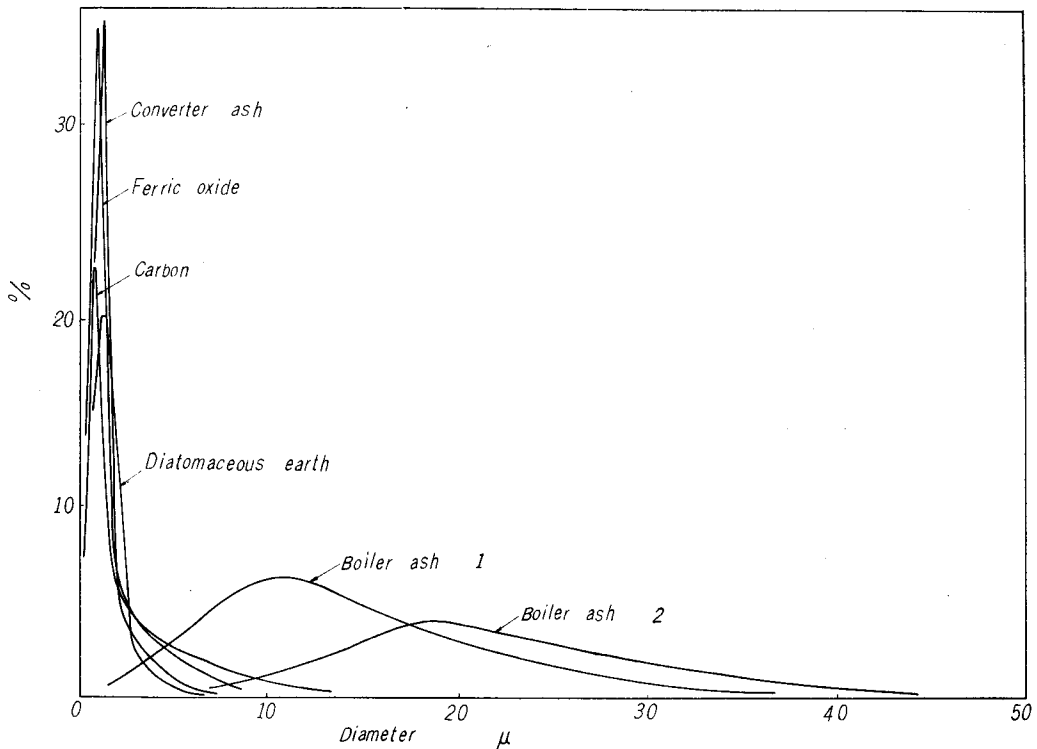


Fig. 6. The diameter distributions of particles used.

gravity, the mean diameter and the experimental temperature range are tabulated in Table 1. Some particles have the circular shape in their projection and others have rectangular shapes or more complicated shapes. When the projection of a particle is similar to a rectangular shape, its diameter  $d_p$  is calculated by the relation<sup>4)</sup>

Table 1.

|                    | Specific gravity<br>kg/m <sup>3</sup> | Mean diameter<br>$\mu$ | Temperature °C |
|--------------------|---------------------------------------|------------------------|----------------|
| Carbon             | 1800                                  | 10.5                   | 990 ~ 1230     |
| Boiler ash 1       | 2000                                  | 13.0                   | 680 ~ 1230     |
| Boiler ash 2       | 2000                                  | 19.5                   | 710 ~ 1270     |
| Ferric oxide       | 3600                                  | 2.34                   | 890 ~ 1270     |
| Converter ask      | 3500                                  | 2.6                    | 850 ~ 1220     |
| Diatomaceous earth | 1750                                  | 5.8                    | 890 ~ 1140     |

$$d_p = \left( \frac{4}{\pi} \cdot 0.75 \cdot BL \right)^{1/2},$$

where  $B$  and  $L$  are the side length of rectangle. The mean diameter is estimated as follows

$$D_m = (\sum n_i d_i / \sum n_i)^{1/3},$$

where  $n_i$  is the number of particles having diameter  $d_i$ .

**(2) Relation between the emissivity of fine particle cloud  $\varepsilon_p$ , the absorption thickness  $v_m S_0$  and the variable  $x_m$**

It is made clear by the above theoretical treatment that the radiative intensity is influenced by the temperature, its distribution, the absorption thickness and the distribution of volumetric concentration. But in the present experiment, the distribution effect of temperature and volumetric concentration, and also the effect of temperature itself are not made clear as a result of the considerable dispersion of the data. The relation between the emissivity of fine particle cloud and the absorption thickness is shown in Fig. 7. It can be seen from Fig. 7 that the emissivity of carbon particle cloud is the highest and those of other particle cloud decrease in the following order of ferric oxide, converter ash, diatomaceous earth and boiler ash, and their differences are very remarkable. From the data of boiler ash 1 and 2, the diameter effect on emissivity is not remarkable. It has been considered generally that the proper character of radiation of solid may change, according as the dimension of the solid approaches to the wave length of radiation. But the above fact seems to show that the proper character of these solid surfaces for the radiative intensity still remains unchanged when the size of particles is in the experimental range, even though it is very small.

From these data the empirical formulae were obtained using the general form

$$\varepsilon = 1 - e^{-K v_m S_0}, \text{ where } K \text{ is constant,}$$

as follows.

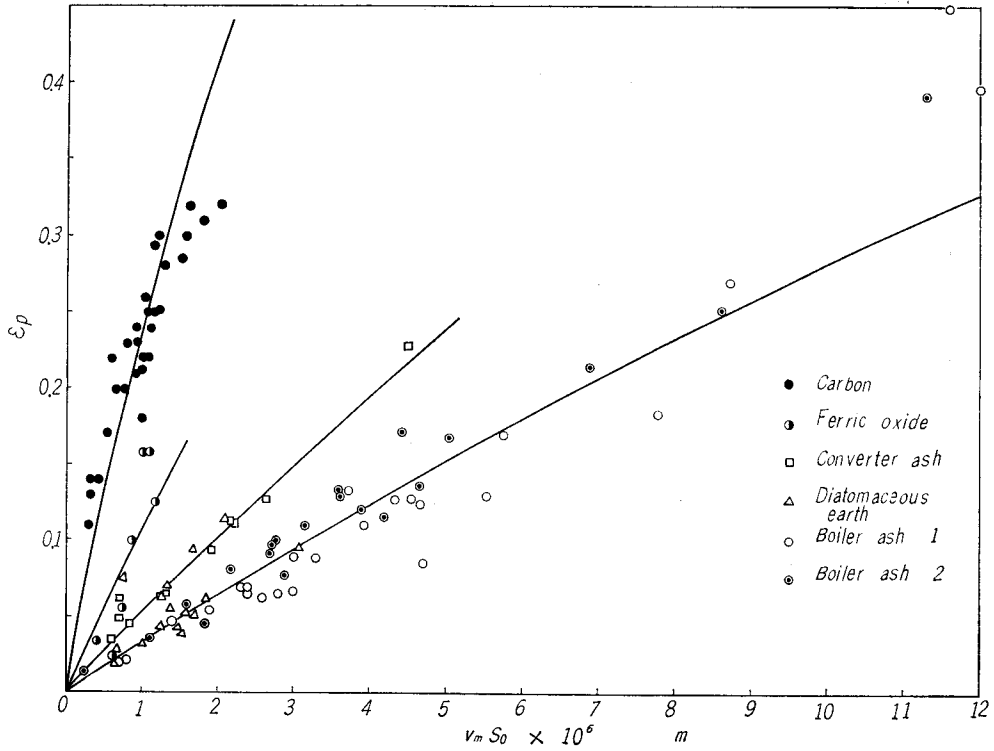


Fig. 7. The relation between the emissivity of fine particle cloud and the absorption thickness.

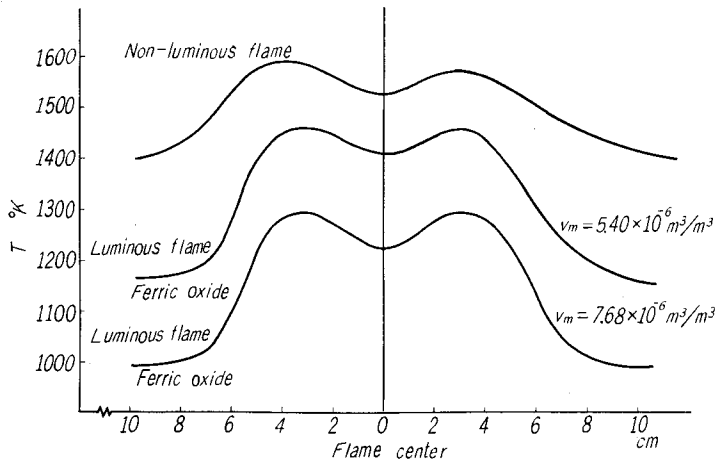


Fig. 8. The temperature distribution of non-luminous flame and luminous flame.

|                                   |  |
|-----------------------------------|--|
| carbon                            | $\epsilon = 1 - e^{-0.268 \cdot 10^6 \cdot \nu_m S_0}$ |
| ferric oxide                      | $\epsilon = 1 - e^{-0.112 \cdot 10^6 \cdot \nu_m S_0}$ |
| converter ash                     | $\epsilon = 1 - e^{-0.054 \cdot 10^6 \cdot \nu_m S_0}$ |
| boiler ash and diatomaceous earth | $\epsilon = 1 - e^{-0.033 \cdot 10^6 \cdot \nu_m S_0}$ |

Solid lines in Fig. 7 show these formulae.

In the present experiment, the temperature is generally low when the absorption thickness is large, as shown in Fig. 8. In the case of boiler ash, it can be seen that the emissivity increases according as the temperature becomes lower. This is explainable by supposing that the radiative intensity of the long wave side is stronger. On the contrary, in the experiment of carbon particle, the emissivity decreases according as the temperature becomes lower, since the radiative intensity of the short wave side is stronger. So, strictly speaking, the above formulae must include the term of temperature effect but it is difficult as the data disperse considerably.

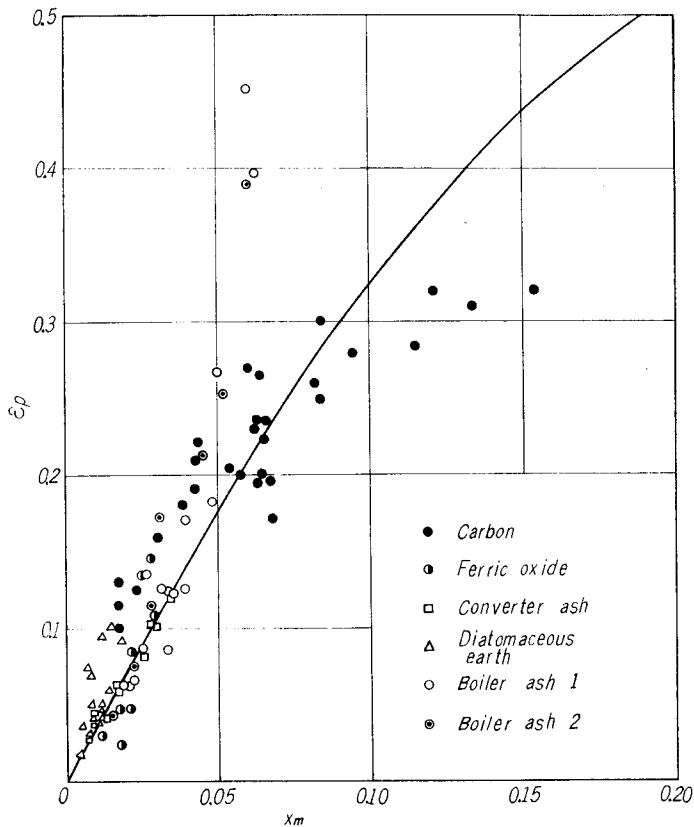


Fig. 9. The relation between the emissivity of fine particle cloud and the variable  $x_m$ .

The relation between the emissivity of fine particle cloud  $\epsilon_p$  and the variable  $x_m$  is shown in Fig. 9, where constants  $k$  are chosen from the data as follows:

|        |              |               |                                      |
|--------|--------------|---------------|--------------------------------------|
| carbon | ferric oxide | converter ash | boiler ash and<br>diatomaceous earth |
| 0.80   | 0.28         | 0.18          | 0.08                                 |

Solid line in Fig. 9 represents Eq. (19). The above-mentioned tendency of the difference of temperature effect between the case of boiler ash and carbon particle is also shown in Fig. 9 more remarkably.

### (3) Relation between the emissivity of particle cloud and that of particle-piled surface

As a method of predicting the emissivity of particle clouds floating in the high-temperature gas, measurements of emissivities of high-temperature particle-piled surfaces were tried. The results are tabulated in the next table.

|                    | Temperature °C | Emissivity |
|--------------------|----------------|------------|
| carbon             | 673            | 0.83       |
| ferric oxide       | 447            | 0.74       |
| diatomaceous earth | 473            | 0.66       |
| boiler ash 2       | 488            | 0.58       |

It is supposed that these values represent the maximum values of the emissivities of floating particle clouds. The emissivities of particle-piled surfaces decrease in the following order of carbon, ferric oxide, diatomaceous earth and boiler ash. This order is equal to that of the data in Fig. 7. But absolute values are not proportional each other. This fact can be interpreted as the effect of the temperature difference, and as the influence of many small gaps or holes existing at the particle-piled surface which may act as blackbody.

## 5. Conclusion

Radiative intensity of fine particle cloud floating in high-temperature gas was treated analytically and the influences of the mean temperature, its distribution, the absorption thickness and the distribution of volumetric concentration were analyzed. On the other hand, the relation between the emissivity of several fine particle cloud and absorption thickness was made clear experimentally. The emissivity of carbon particle cloud is the highest and the emissivity of other particle clouds used decreases in the following order of ferric oxide, converter ash, diatomaceous earth and boiler ash. For

each particle, empirical formulae were obtained. As the differences among them are very remarkable, it is supposed that the proper character of the radiation of solid surface remains unchanged even though the dimension of the particles approaches to the wave length of radiation. The order of the magnitude of emissivities of those particle-piled surfaces is found to agree with that of the emissivities of those particle clouds floating in high-temperature gas.

#### References

- 1) A. Schack : Z. Tech. Phys., **6** (1925).
- 2) T. Sato and R. Matsumoto : Trans. JSME., **26**, 177 (1961-5).
- 3) W. H. Giedt : Principles of Engineering Heat Transfer.
- 4) S. J. Gregg : The Surface Chemistry of Solids.